communications earth & environment

Article

https://doi.org/10.1038/s43247-025-02016-7

Chronic nitrogen legacy in the aquifers of China

Xin Liu[1,2], Fu-Jun Yue[1,3] ✉, Li Li[4], Feng Zhou[5,6], Hang Wen[1], Zhifeng Yan[1], Lichun Wang[1], Wei Wen Wong[2], Cong-Qiang Liu[1,3,7] & Si-Liang Li[1,3,7] ✉

About half of the global drinking water comes from groundwater, yet groundwater quality is threatened by high nitrate concentrations globally. Our understanding of groundwater nitrate concentrations is often limited by inaccessibility of groundwater and scarcity of nitrate data in groundwater. Here we used machine learning and decision tree-heatmap analysis by compiling nitrate concentrations and isotope data from 4047 groundwater sites across China to understand their dynamics and drivers across gradients of geographical, climate, and human factors. Results show that nitrate concentrations vary substantially over depth and are generally lower in deeper groundwater, indicating potentially higher nitrate removal rates according to nitrate isotopic pattern such as denitrification at depth. At similar groundwater aquifer depths, nitrate concentrations are highest in urban regions with high population density. In addition, nitrate concentrations are generally higher in arid northern China than humid southern China. Interestingly, while groundwater nitrate concentrations are lower at deeper depths, slow groundwater flow also indicates prolonged nitrogen legacy. Although there has been an overall decline in groundwater nitrogen pollution in China since 2016, persistent pollution has lingered. Future strategies for groundwater quality protection in China should address the long-term legacy of nitrate in different aquifers and rising nitrogen levels in groundwater.

Clean water and sanitation are essential to the society, as discussed in The United Nations' Sustainable Development Goals (SDGs)[1–4]. Groundwater is a major freshwater resource that provides half of the drinking water available to the global population[5,6]. This number can increase by up to 70% and 95% for urban and rural residents of China, respectively[7]. Increasing population and expanding agriculture have continued to threaten global groundwater resources[5,8]. Groundwater nitrogen (N) accumulation has been reported globally, including in China[9], Germany[10], India[11], and the United States[12]. Excessive reactive nitrogen, primarily nitrate, has caused cascading effects on ecosystem instability, groundwater degradation, and human health[13]. Although nitrate removal from groundwater has been achieved in some regions at considerable cost[14,15], high nitrate concentrations in groundwater remain a serious and widespread issue, particularly in developing countries. Understanding whether this upward trend will persist due to ongoing development and the intensified use of agriculture is of paramount importance[16,17].

Globally, agriculture and wastewater discharge are responsible for high nitrate concentrations in groundwater[18,19], except in regions with naturally occurring nitrate from bedrock[20]. Although nitrogen fertilizers have historically been the primary contributor to high nitrate concentrations in groundwater[21], the contribution of wastewater has gained growing importance with expanding urbanization[22]. In addition, changing environmental conditions across diverse aquatic ecosystems, including changing climate and intensifying anthropogenic activities[23,24], could potentially modify nitrogen input and the pathways of reactive nitrogen[25,26], which further complicates our understanding of nitrate dynamics in groundwater. Discerning the distinct impacts of individual influential factors remains a significant challenge, partly due to inadequate large-scale groundwater sampling and data. In addition, extrapolation of understanding from local-scale studies to regional or continental levels poses an elusive challenge.

Groundwater stores large quantities of nitrogen and facilitates its transport, transformation, and accumulation[27–29]. However, the spatial

[1]Institute of Surface-Earth System Science, School of Earth System Science, Tianjin University, Tianjin, China. [2]Water Studies, School of Chemistry, Monash University, Melbourne, Australia. [3]Tianjin Key Laboratory of Earth Critical Zone Science and Sustainable Development in Bohai Rim, Tianjin University, Tianjin, China. [4]Department of Civil and Environmental Engineering, Pennsylvania State University, University Park, State College, USA. [5]Laboratory for Earth Surface Processes, Ministry of Education, College of Urban and Environmental Sciences, Peking University, Beijing, China. [6]College of Geography and Remote Sensing, Hohai University, Nanjing, China. [7]Haihe Laboratory of Sustainable Chemical Transformations, Tianjin, China. ✉e-mail: fujun_yue@tju.edu.cn; siliang.li@tju.edu.cn

relationship between groundwater aquifer depth and nitrogen dynamics has rarely been characterized. Hence, understanding the effect of aquifer depth on groundwater nitrogen dynamics is essential to reveal mechanisms that regulate groundwater nitrate and groundwater quality. Nevertheless, it is challenging to obtain accurate data on aquifer depth and groundwater nitrate dynamics at a large scale[9]. Fortunately, wells have been the most extensive and direct way of withdrawing groundwater since ancient times, and their widespread distribution across China provides a promising avenue for investigating the dynamics of nitrate in groundwater. The main reasons are as follows: natural convenience for groundwater sampling; moreover, groundwater nitrate dynamics have been extensively investigated throughout China since 2000, and previous studies have shown that groundwater table can serve as a representative measure of local aquifer depth in numerous regions[30,31]. Therefore, it is reasonable and innovative to study the role of aquifer depth in nitrate dynamics by using well data.

Here, we compiled and analyzed available data on nitrate concentrations and isotopic data in groundwater across gradients of geographical features, climate zones, and economic regions in China. We aimed to answer the following questions: (1) What is the spatial pattern of groundwater nitrate concentrations in China? (2) How do the nitrate concentrations in groundwater vary with aquifer depth? (3) How do climate conditions, geography, and anthropogenic activities interact to influence nitrogen concentration in groundwater? We examined the influence of various factors, including groundwater aquifer depth, hydrochemical characteristics, land use, ecoregion, latitude, longitude, population density (PD), mean annual precipitation (MAP), and mean annual temperature (MAT). The results provide comprehensive datasets and identify influential drivers of nitrate dynamics in groundwater. The outcome of this study can provide valuable insights not only for managing nitrogen pollution in groundwater but also for offering theoretical support for developing groundwater quality management strategies that subsequently contribute to informed decision-making on both national and global scales.

Results and discussion

The dynamics of nitrate concentrations in groundwater across China

The depths of groundwater aquifer range from 0 to 860 m (Fig. 1). The average depths of the groundwater in lowlands, middlelands, and highlands are 83.0 ± 127.5 m (Mean ± SD), 62.7 ± 75.4 m, and 23.3 ± 51.0 m, respectively (Table S1). Statistical data demonstrated that the groundwater aquifer depths in southern China are generally shallower than those in northern China due to higher precipitation levels and shallow groundwater tables in southern China (Fig. 1a).

Nitrate concentrations (Unless otherwise specified, represents NO_3^- rather than $N\text{-}NO_3^-$ in this study) ranged from 0 to 824.6 mg L^{-1} (31.2 ± 69.4 mg L^{-1} (Mean ± SD); median: 9.0 mg L^{-1}), exceeding previous reports by Gu et al.[9] (10.9 ± 18.1 mg L^{-1} in groundwater in China) and Ioannis et al.[13] (5.5 ± 5.1 mg L^{-1} in global groundwater). Among them, concentrations are highest in shallow groundwater, reaching 824.6 mg L^{-1} (70.3 ± 136.6 mg L^{-1}). Geographically, nitrate concentrations exhibited significant spatial variation, with relatively higher concentrations in northern China than in southern China (Fig. 1a and Table S1). The economic regions in northern China (NC, MYR, and NE) exhibited the highest mean nitrate concentration. Notably, NC stands out at a mean concentration of 56.8 ± 104.6 mg L^{-1}, aligning with its highly developed economy (Fig. 1b). In addition, lowlands with dense population displayed higher average nitrate concentration (36.1 ± 76.7 mg L^{-1}) compared to the middlelands and highlands. Groundwater nitrate concentrations also changed with land use types. As expected, groundwater in regions with minimal disturbance exhibited significantly lower concentrations compared to those in cropland and urban regions (Fig. 1d). Aside from water quality variables (TDS), MAP and MAT are the second most important attributes driving nitrate concentrations, indicating the importance of climate control on solute concentrations[32]. This is also consistent with nitrate concentrations in rivers, for example, in the United States[33], although mean nitrate concentrations of groundwater aquifers are usually higher in croplands. Similarly, regions with higher population densities showed slightly elevated nitrate concentration, which could be attributed to increased nitrogen load (Fig. 1e).

We used geospatial machine learning (i.e., random forest model) based on predictor datasets (Table S2) and generated nitrate concentrations across China at a spatial resolution of 0.05° × 0.05° (Fig. 2). The model performed well ($R^2 = 0.53$ and NSE = 0.50). The map identified more severe nitrate pollution in northern China than in southern China (Fig. 2a). For instance, the groundwater of agricultural regions (such as North Coast and Guanzhong plain) and urban regions (such as Beijing, Tianjin, and Guangdong-Hong Kong-Macao Greater Bay Area) face a greater threat of nitrate than natural land. In addition, model uncertainty was assessed using the ML model. High uncertainty was mainly concentrated in regions with limited measurements, such as the Qinghai-Tibet Plateau, northeastern China, and Yunnan Province (Fig. 2b). In contrast, regions with abundant observations can significantly reduce model uncertainty, such as the Yellow River Basin and Yangtze River Basin. Note that, large uncertainty is also observed in regions with low concentrations, such as Yunnan Province, indicating the limitation of model capacity in regions with lower values[34]. Overall, more field measurements of nitrate concentrations are required to reduce prediction uncertainty in hotspot regions.

Nitrate concentrations decrease with groundwater aquifer depth

In contrast to existing studies that predominantly examined nitrogen concentrations at individual sites[35,36], this study examined spatial variation and interconnected patterns of nitrate concentration in groundwater. Among all hydrochemical characteristics and other influencing factors, aquifer depth exerted the most predominant influence on nitrate concentration in groundwater (Fig. 1c and Fig. 3a–e). Nitrate concentrations decreased with increasing aquifer depths ($R^2 = 0.34$, $P < 0.001$) (Fig. 3c). This general pattern was also evident in North China, where aquifer depth and nitrate concentrations varied tremendously (Fig. S1a). $\delta^{15}N\text{-}NO_3^-$ increased and then decreased with increasing aquifer depth, peaking at about 8 m (Fig. 3d), suggesting that nitrate may have undergone two distinct biogeochemical stages. The first is that more anoxic conditions are coupled with increasing carbon sources (e.g., DOC) (Fig. S2a), resulting in a greater denitrification with increasing depth. The subsequent decline may be attributed to declining microbial abundance and carbon and nitrogen sources with increasing aquifer depth[37]. Values of $\delta^{18}O\text{-}NO_3^-$ continued to increase, but also showed minimum values at peak values of $\delta^{15}N\text{-}NO_3^-$ (Fig. 3e), which may be attributed to processes including water evaporation, which enriched $\delta^{18}O_{water}$ and subsequent isotopic fractionation during nitrification[13]. These changes in nitrate dynamics and isotopes indicate combined influence of multiple drivers, which will be discussed in the subsequent section.

Values of $\delta^{15}N\text{-}NO_3^-$ and $\delta^{18}O\text{-}NO_3^-$ varied with aquifer depth but the correlations were insignificant (ANOVA, $P > 0.05$). Values of $\delta^{15}N\text{-}NO_3^-$ were lowest in shallow (CV = 1.03, <20 m) to very deep groundwater (CV = 0.40, >100 m), which may be caused by the diverse nitrate sources and/or varying degrees of biological activities[38]. Although the majority of samples fell within the theoretical range of nitrification (indicated by the box regions in Fig. S3a–d), some were outside this range, suggesting the potential role of other processes such as denitrification in regulating nitrate concentrations[39]. The lack of a discernible relationship between $\delta^{15}N\text{-}NO_3^-$ and $1/NO_3^-$ in groundwater at different depths (Fig. S3e–h) implies that the $\delta^{15}N\text{-}NO_3^-$ is likely influenced by multiple sources and multiple biological removal processes[40]. Meanwhile, the $\delta^{15}N\text{-}NO_3^-$ and $Ln(NO_3^-)$ were negatively correlated (Fig. S3i–l), especially in shallow groundwater (<20 m, Fig. S3i), indicating the occurrence of biological removal processes[41]. Therefore, groundwater biogeochemistry, including nitrification and denitrification, may play a key role in regulating N dynamics and turnover within groundwater.

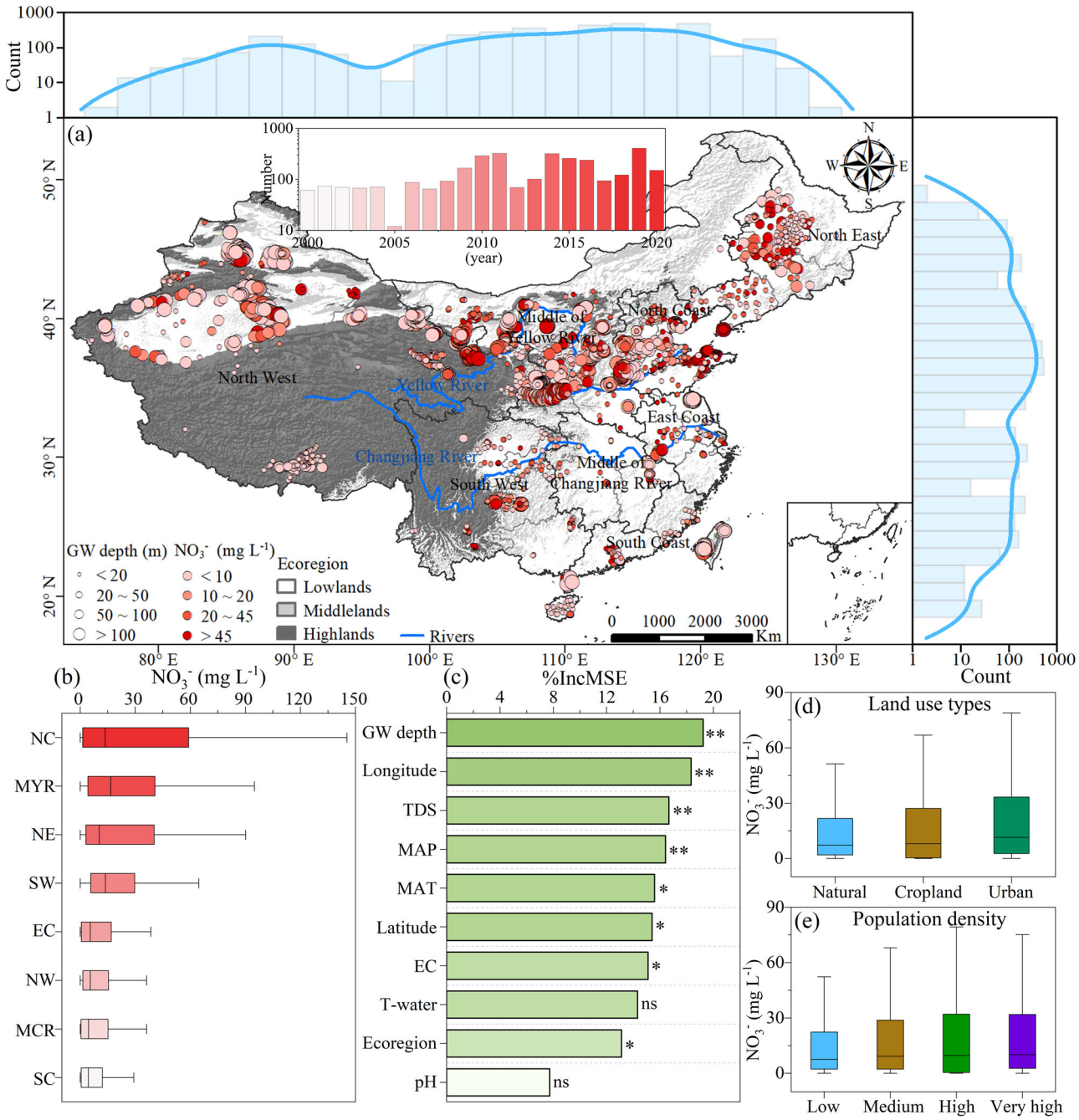

Fig. 1 | The spatial variation of nitrate concentrations in 4047 groundwater sites in China. a The upper and right subgraphs show the counts of longitude and latitude distributions of the sample sites, respectively. The red bar chart above the map shows the number of sampling points in different years. **b** Mean concentrations of nitrate in eight economic regions: North Coast (NC), Middle of Yellow River (MYR), North East (NE), South West (SW), East Coast (EC), North West (NW), Middle of Changjiang River (MCR), and South Coast (SC). **c** The relative importance of influential drivers for groundwater nitrate concentrations was determined by regression forecasting using random forests. The columns marked * ($P < 0.05$) and ** ($P < 0.01$) indicate that drivers have significant impacts on nitrate concentrations, while ns ($P > 0.05$) indicates that drivers have no significant differences in nitrate dynamics. **d**, **e** Nitrate concentrations under different land use types and population densities, respectively (classification methods in "Materials and Methods"). The box plots include three modules: box limits, upper and lower quartiles; small cube, average value; center line, and median.

Groundwater nitrate sources

To quantify the contribution of different sources to nitrate, we used a Bayesian stable isotope mixing model (MixSIAR). We considered atmospheric deposition, manure & sewage, soil nitrogen, and chemical fertilizer[41,42] to estimate the potential end-members contributing to nitrate in groundwater (Table S3). The model results showed that nitrate in groundwater primarily originated from soil nitrogen, manure & sewage, accounting for 38.4 ± 23.0% and 31.8 ± 13.4%, respectively (mean ± SD); atmospheric deposition contributed only a small fraction (10.4 ± 3.3%). The contribution of soil nitrogen was greatest in shallow (44.5 ± 22.9%), deep (44.1 ± 26.7%), and very deep groundwater (40.5 ± 23.3%), whereas manure & sewage dominated the nitrate pool in medium groundwater (44.3 ± 22.1%) (Table S4).The unexpected dominant presence of manure & sewage in medium groundwater may be linked to irrigation practices from the 1970s, when manure & sewage were commonly used, although these practices are much less common in China today[43]. The spatial distribution of

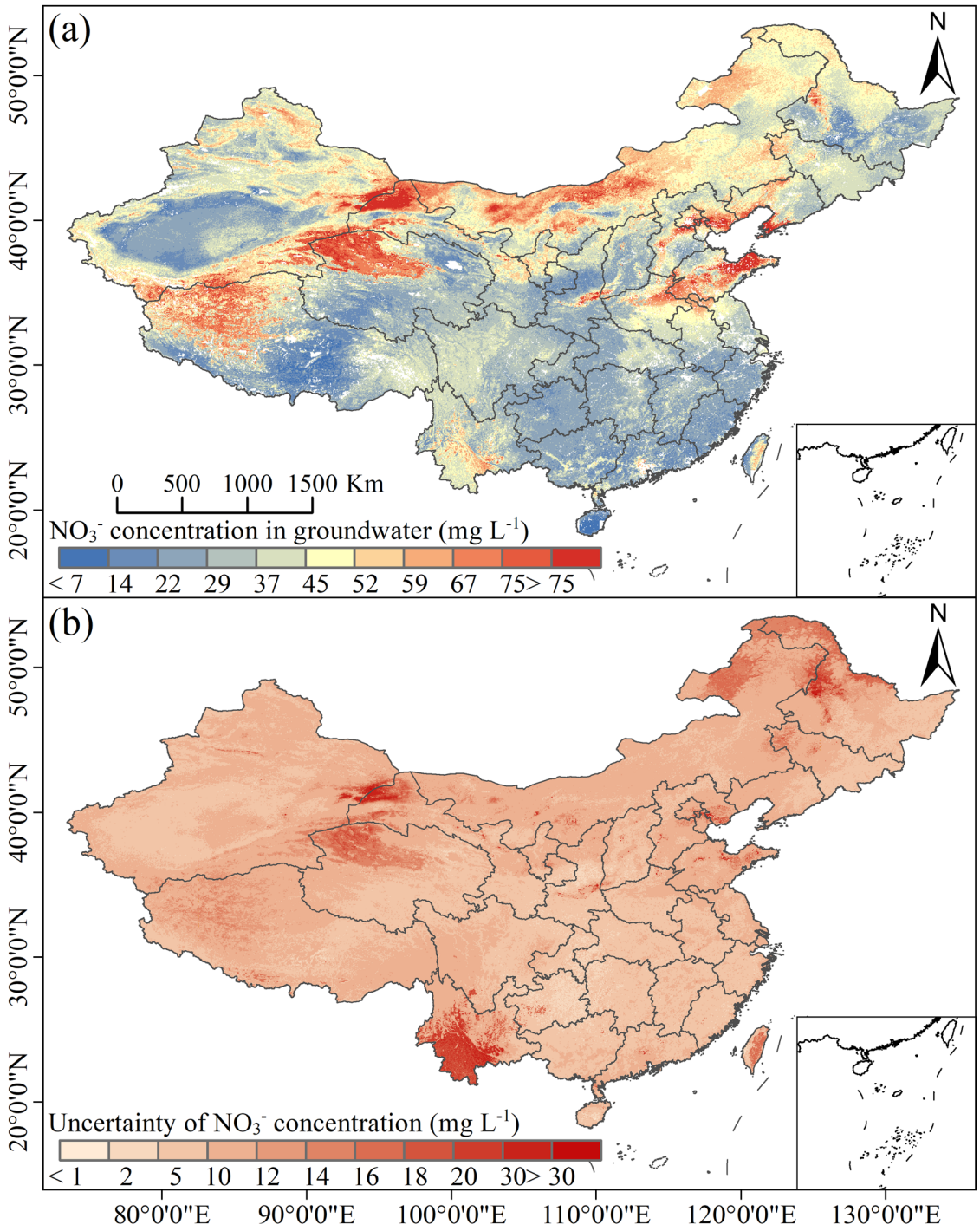

Fig. 2 | Nitrate dynamics in Chinese groundwater. a Simulated nitrate concentrations and (**b**) uncertainty in Chinese groundwater using a machine learning algorithm (random forest modeling), predicted by 66 spatially continuous environmental variables (Table S2). The nitrate values were grouped into 11 categories to generate a color gradient (on the right), where blue and red colors represent low and high values, respectively.

nitrogen input to subsurface system varies across ecoregions. For example, in North China, groundwater nitrogen often predominantly originates from manure & sewage (65.1%), with soil nitrogen, atmospheric deposition, and chemical fertilizer contributing 18.0%, 9.3%, and 7.6%, respectively[44]. Conversely, in South West, groundwater nitrate is derived more from chemical fertilizer (32%) than soil nitrogen, atmospheric deposition, and manure & sewage, contributing 25%, 18%, and 25%, respectively[45].

The uncertainties of sources proportion of nitrate in groundwater during calculation would be caused by multi sources mixing and various transformation processes with different isotopic fractionation[41]. The high soil nitrogen contribution may reflect more samples from croplands than from other land use types (Table S4). As has been discussed extensively in literature (e.g., Van Meter et al.[18]), agricultural lands have accumulated nitrogen originating from nitrogen fertilizers, manure, and other organic materials for decades to centuries[46]. The data here potentially indicate that the accumulation of legacy soil nitrogen contributed more to the observed nitrate than the more recent addition of fertilizer and atmospheric addition. Thus, when nitrogen inputs are reduced, the nitrogen accumulated in soil organic matter may still be released and transported to aquifers, contributing to the nitrogen legacy in groundwater[18,47]. This also indicates that

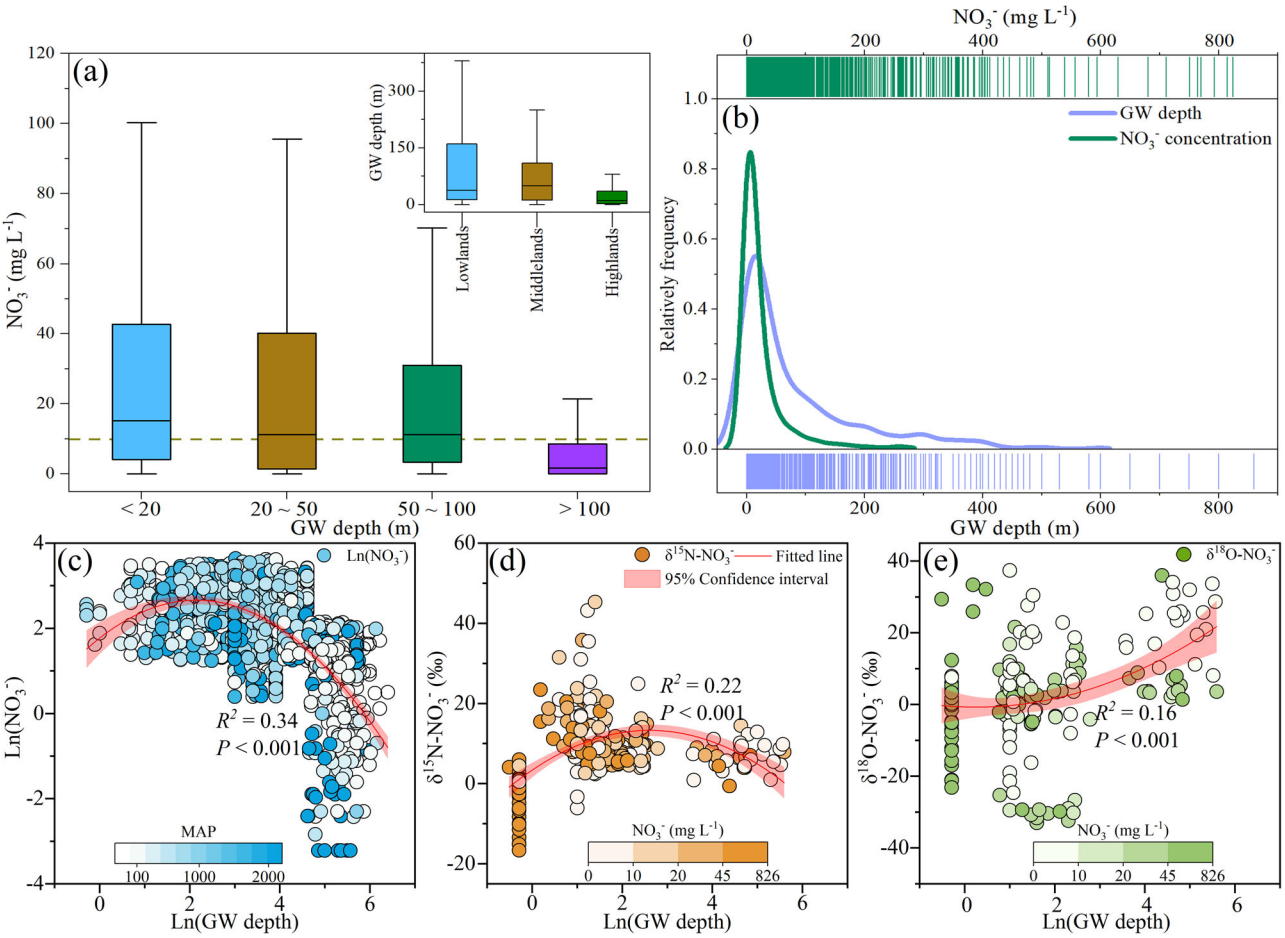

Fig. 3 | Nitrate concentrations, isotopes, and groundwater aquifer depth. **a** Nitrate concentrations at various aquifer depths and elevations. **b** The frequency distribution of NO_3^- concentrations and aquifer depths. **c** NO_3^- concentrations, including only samples in the first to third quartile nitrate concentrations for the four classes of aquifer depths, (**d**) $\delta^{15}N\text{-}NO_3^-$, (e) $\delta^{18}O\text{-}NO_3^-$ as a function of aquifer depth. Nitrate concentrations generally decreased with increasing depth and MAP (**c**); values of $\delta^{15}N\text{-}NO_3^-$ peak, whereas those of $\delta^{18}O\text{-}NO_3^-$ reach lowest values at some intermediate depths (**d**, **e**).

neglecting groundwater nitrogen isotope fractionation may lead to source blurring and inaccurate results. For example, although the $\delta^{15}N\text{-}NO_3^-$ values for N fertilizers are approximately 0‰, the volatilization of ammonia can introduce a bias of about 2‰, which may increase to as much as 4‰ when crops first absorb and then degrade[48,49].

Chronic pollution prolongs in North China and Middle Yellow Rivers

A comprehensive understanding of the dynamic relationships among influencing factors, groundwater aquifer depth, and nitrate dynamics is a prerequisite for the management of the global groundwater system[27,50]. The correlations among aquifer depth, geographical location, and climate may reflect an intrinsic relationship between aquifer depth and nitrate dynamics (Fig. 4). When the aquifer depth was greater than 140 m, most groundwater had low nitrate concentrations, whereas groundwater below 140 m in lowlands and middlelands with high population density often had medium (7.5%) and poor (8.8%) water quality, as measured by nitrate concentrations (Fig. 4a). It should be noted that in middlelands with both very high and low populations, the groundwater quality deteriorates significantly to a poor level (35%) when aquifer depth ranges from 0 to 18 m (Fig. 4a), which may be attributed to more recent nitrogen inputs[9]. According to the threshold of aquifer depth, Class I groundwater (≤140 m, 75.8%) was mainly located in lowlands (53.5%) and middlelands (33.0%), with cropland being the dominant land cover (49.4%). However, less than half of the groundwater (44.8%) met the water quality standard of 10 mg L^{-1} (Fig. S4). In contrast, Class II groundwater (>140 m, 24.2%) was mainly situated in lowlands (71.0%) and middlelands (22.8%), characterized by high population density levels (55.8%) and urban land cover types (44.0%), and the overall water quality was excellent (82.4%) (Fig. S4). Additionally, the threshold for nitrate dynamics under different influencing factors showed that most Class II groundwater (>140 m) is classified as excellent, whereas there is significant variability in the nitrate dynamics of Class I groundwater (≤140 m) (Fig. 4a and Fig. S4), highlighting the substantial impact of anthropogenic activities[33]. Note that, there are two turning points in nitrate dynamics as aquifer depth increases, one of which is the turning point shown in Fig. 3e (aquifer depth ca. 8 m), while the other is the threshold from decision tree-heatmap (Fig. 4a, aquifer depth ca. 140 m). This indicated that anthropogenic activities have impacted depths of up to ca. 140 m (i.e., Class I groundwater), and denitrification has concurrently affected shallow groundwater (≤8 m) owing to abundant carbon sources[51]. This information can provide theoretical support for sustainable future groundwater quality management by explaining why shallow groundwater is more susceptible to high nitrates level.

The association among auxiliary data (including geographical, climatic factors, and hydrochemical characteristics), aquifer depth, and nitrate concentration using structural equation model showed interesting relationships (Fig. 4b, c). TDS (λ = 0.61), EC (λ = 0.44), and geographical factors (λ = 0.26) exhibited positive effects on nitrate, whereas aquifer depth (λ = −0.15) and T-water (λ = −0.14) showed negative effects. Furthermore, the total effect of climate factors (λ = 0.40) on nitrate was the highest, wherein the indirect effect of aquifer depth (λ = −0.22) and climate factors (λ = 0.46) surpassed the direct effect. However, the direct

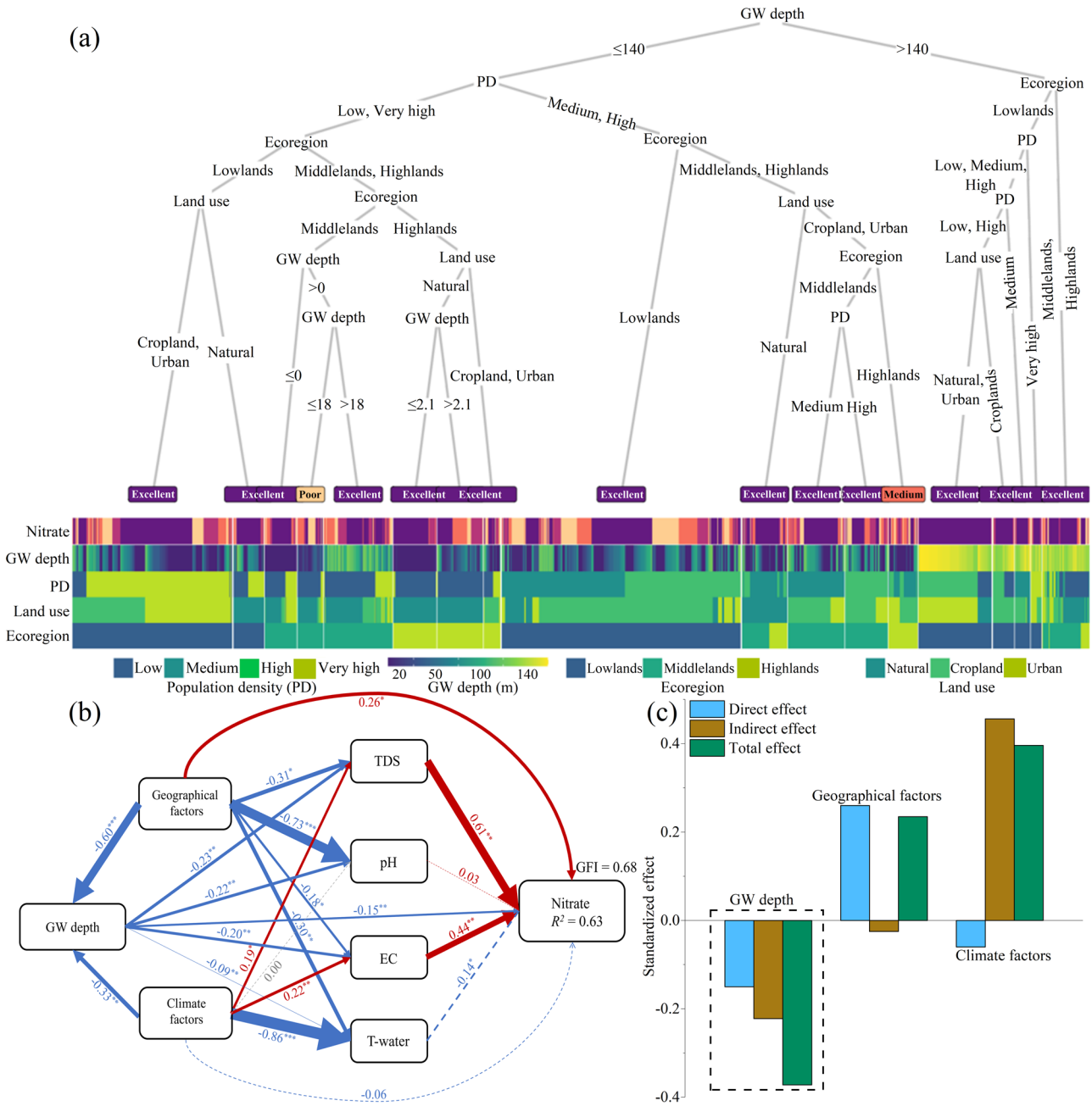

Fig. 4 | The relationships between groundwater nitrate concentrations and influencing factors, including groundwater aquifer depth, geographical factors (including ecoregion, latitude, and longitude), and climatic factors (including MAP and MAT). a A decision tree-heatmap for predicting the threshold for nitrate concentration based on environmental factors associated with anthropogenic activities. **b**, **c** Structural equation models describing the direct, indirect, and total effects of aquifer depth, geographical factors, climate factors, and hydrochemical characteristics of nitrate. Path coefficients (i.e., regression coefficient) and coefficients of determination ($R^2 = 0.63$) represent the effect size (λ) of the relationship (numbers adjacent to the paths) and the proportion of variance explained by the relationships in the model. The direct effect represents the impact of the independent variable on dependent variable, while indirect effect reflects its influence through one or more intermediate variables. The total effect is the combined effect of independent variable on dependent variable, which is the arithmetic sum of direct and indirect effects. The thickness of the arrows reflects the relative magnitudes of the standardized path coefficients. Red, blue, and gray color denotes positive, negative, and irrelevant effects, respectively. The dashed lines represent insignificant relationships; $^*P < 0.05$, $^{**}P < 0.01$, and $^{***}P < 0.001$.

effect of geographical factors (λ = 0.26) remained greater than the combined indirect effects.

Groundwater nitrate concentrations were predominantly controlled by environmental factors, especially climate factors indirectly[32,52,53] (Fig. 4c). Climatic conditions, including temperature and precipitation, can significantly influence the contact time between water and nitrogen-binding soils, thereby facilitating transformation of nitrate into other forms via processes such as denitrification[54,55]. Sadayappan et al.[33] found that arid climate can elevate nitrate concentrations in water by reducing its transport and transformation through lower water content and flow, even without human-induced nitrogen inputs. The influence of climatic factors on nitrate dynamics was achieved through indirect processes (Fig. 4c) and biogeochemical reactions. Munz et al.[56] demonstrated that temporal variations in temperature and redox zonation dominate the migration and degradation of nitrate within groundwater aquifer, which is also verified by the relationship between Oxidation-Reduction Potential (Eh) and NO_3^- in this study (Fig. S2b).

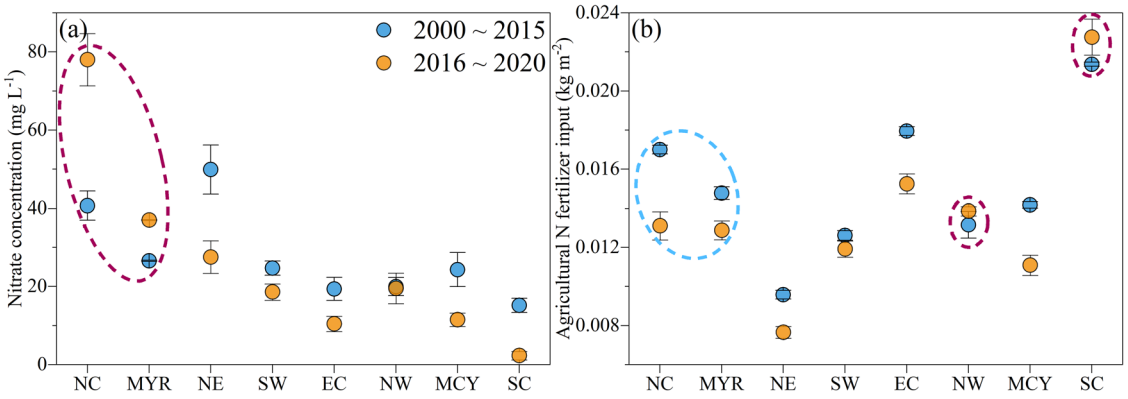

Fig. 5 | Regional-level changes in groundwater nitrate concentration and agricultural N fertilizer input for 2000–2015 and 2016–2020. a Comparison of groundwater nitrate concentrations in eight economic regions in 2000–2015 and 2016–2020. **b** Comparison of per-unit agricultural N fertilizer input in eight economic regions in 2000–2015 and 2016–2020. This broad spatial coverage is crucial for capturing the major regional trends in nitrogen pollution, adequately representing the two distinct periods. Blue circles and yellow triangles indicate the 2000–2015 and 2016–2000, respectively. Blue shading (and red ellipse) represents the value of 2016–2020 is higher than that of 2000–2015, and vice versa in green shading (and blue ellipse).

In addition, more humid regions with higher precipitation had lower nitrate concentrations at similar depths (Fig. 3c). To further explore this, we compared North Coast, which has a more arid climate, and South West which has much more precipitation. They also exhibited distinct agricultural practices, lithologies, varied aquifer depths and nitrate dynamics (Fig. S1). The $\delta^{18}O\text{-}NO_3^-$ enrichment differs between NC and SW, with isotopic enrichment occurring more in NC as aquifer depth increases in a more arid climate but not as much in humid SW (Fig. S1). The observed isotopic enrichment of $\delta^{18}O\text{-}NO_3^-$ in NC with deeper groundwater likely arose from greater evaporation[13]. In contrast, this does not occur as much in the humid SW[57]. In effect, low precipitation in NC probably reduces transport and nitrogen use efficiency[28,44]. In contrast, in wet and rainy SW, abundant rainfall throughout the year facilitates the leaching of legacy nitrogen, as well as the utilization of nitrogen fertilizers through more sufficient soil mositure[58,59]. Although widespread irrigation practices are present in NC, they are primarily concentrated during the crop growing seasons[60]. For many years, soil moisture has remained relatively low, limiting the transformation and mobility of soil nitrogen. This intermittent moisture availability may further restrict soil nitrogen transport and processing, contributing to lower nitrogen use efficiency outside the irrigation periods[59]. This is consistent with the general conclusion that solute concentrations tend to be higher in arid climate and lower in humid climate[32]. That study examined concentrations of 16 solutes, including nitrate, at hundreds of sites in the United States. The lower concentrations in humid climate were attributed to more rapid solute export from the systems (both surface water and groundwater). The influence of climate on nitrate concentrations in inland waters, especially groundwater, is generally underestimated in literature. Data from the present study highlight the important role of climate in groundwater nitrate concentrations.

Unlike climatic factors, geographical factors had a direct impact on groundwater nitrate concentrations (Fig. 4c). The distribution of ecoregions, location, and population density determine land use types, which significantly affect nitrogen input across various land use types. Nakagawa et al.[61] and Sadayappan et al.[33] identified land use as the most significant factor affecting nitrate concentrations in rivers. Groundwater in urban and cropland had higher nitrate concentrations (Fig. 1d), similar to observations for riverine nitrate concentrations in Zhi and Li[62]. Moreover, different developmental and anthropogenic activities also affect nitrate concentration in different regions. There is a roughly linear relationship between NO_3^- and agricultural N fertilizer ($R^2 = 0.11$, $P < 0.001$), TN wastewater ($R^2 = 0.29$, $P < 0.05$), and ammonia wastewater ($R^2 = 0.11$, $P > 0.05$) across eight economic regions (Fig. S5). Further analysis revealed that nitrate concentration in NC economic region significantly deviated from the fitting line for both agricultural N fertilizer and ammonia N wastewater (Fig. S5). This suggests that nitrate concentrations are primarily influenced by industrial and domestic wastewater, especially TN wastewater, rather than by agricultural activities. For groundwater in cropland, high nitrate concentrations resulted from N legacies due to low nitrogen use efficiency[63]. The global average nitrogen use efficiency was 0.46 in 2010[64], and has remained below 0.3 until 2011 in China, the world's largest nitrogen fertilizer consumer[65]. Agricultural activities and wastewater discharge containing nitrogen are important drivers of global groundwater N enrichment[27,41].

Statistics indicated a consistent increase in the discharge of TN and ammonia wastewater prior to 2015 (Fig. S6). In response, the Chinese government implemented a series of comprehensive treatment measures in 2015, such as improving wastewater treatment that effectively mitigated this trend[66]. Although the data used in this study is based on single sampling events, the data points across different economic zones are widely distributed during both 2000–2015 and 2016–2020 (see numbers of samples in different economic zones from 2000 to 2020 in Fig. 1a and Table S5). To better capture the temporal variations, we also calculated the overall means and standard deviations (SD) for the two periods: 2000–2015 and 2016– 2020 (Fig. 5). Notably, overall groundwater nitrogen pollution significantly declined during 2016–2020 compared to the data from 2000–2015, except in the NC and MYR (Fig. 5a). This is due to the significantly deeper groundwater in these two regions compared to other regions, such that they do not yet reflect the short-term nitrogen control measures. In other words, it would take longer time for nitrogen management practices to be effective for deeper groundwater[18]. This reflects the complexity of transport and the persistence of legacy nitrogen, reinforcing the notion that recovery is gradual and varies depending on soil depth, land use, and hydrogeological characteristics[52,67,68]. There has been a significant reduction in agricultural nitrogen input in these two regions (Fig. 5b), indicating that the current agricultural treatment measures will have positive implications for the mitigation of groundwater nitrogen pollution in the future. However, rising populations and living standards may intensify the impacts of groundwater nitrate legacy.

Biogeochemistry shapes nitrate dynamics at different aquifer depths

The random forest analysis suggested that groundwater aquifer depth was the primary factor affecting the spatiotemporal variations in groundwater nitrate dynamics (Fig. 1c). The influential factors were ranked as follows: groundwater aquifer depth (GW depth), longitude, total dissolved solids (TDS), mean annual precipitation (MAP), mean annual temperature (MAT), latitude, electrical conductivity (EC), water temperature (T-water), ecoregion, and pH. Although there was a significant range in aquifer depth (0–860 m) and nitrate concentration (0–824.6 mg L^{-1}) (Fig. 3b), nitrate

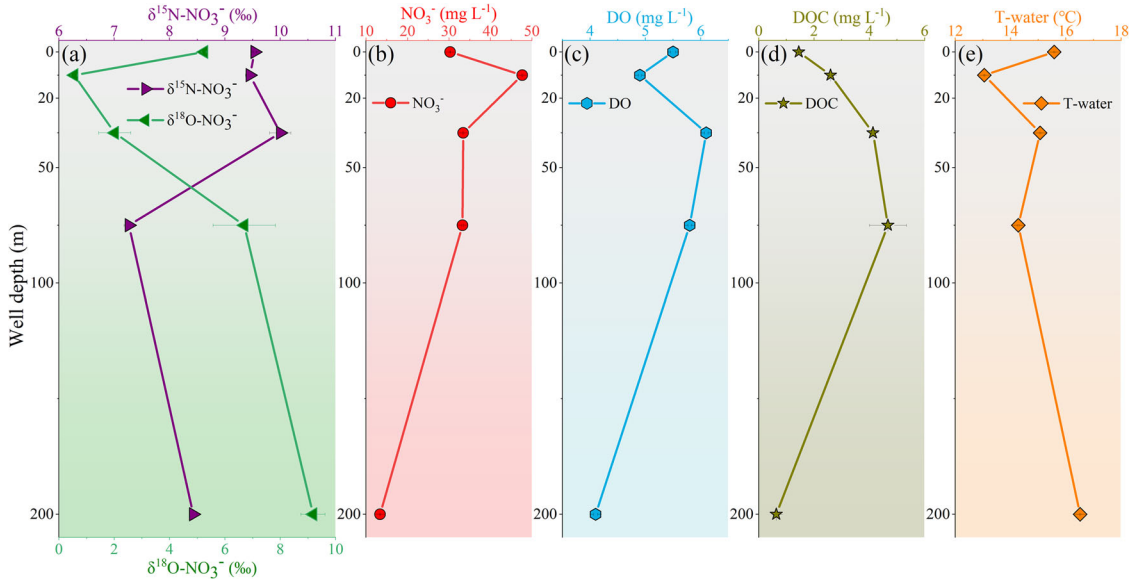

Fig. 6 | Vertical distributions of the mean values of $\delta^{15}N\text{-}NO_3^-$, $\delta^{18}O\text{-}NO_3^-$, NO_3^-, DO, dissolved organic carbon (DOC), and T-water in shallow (<20 m), medium (20–50 m), deep (50–100 m), and very deep (>100 m) from different locations across China. a $\delta^{15}N\text{-}NO_3^-$ (‰; N = 525) and $\delta^{18}O\text{-}NO_3^-$ (‰; N = 401) at different depth. **b** NO_3^- concentrations (mg L^{-1}; N = 4047) at different depths. **c** DO (mg L^{-1}; N = 689) at different depths. **d** DOC (mg L^{-1}; N = 278) at different depths. **e** T-water (°C; N = 1592) at different depths. Values are presented as mean ± SEM (Standard Error of Mean).

concentrations were generally lower in deeper groundwater (Fig. 3c), highlighting the importance of depth in influencing nitrate concentrations[36].

In theory, shallow groundwater with a short retention time[69] and vegetation uptake[51] offers more efficient removal of nitrogen pollution compared to deep groundwater. However, shallow groundwater also receives more nitrogen input from anthropogenic activities and is more susceptible to external environmental factors, as indicated by the higher anthropogenic N sources in shallow groundwater than in medium-depth groundwater (Fig. 6 and Table S4). The highest mean nitrate concentrations in shallow groundwater can be attributed to large nitrogen inputs from external environment[70] and the presence of dissolved oxygen (DO) and nitrifying bacteria in shallow groundwater, which can transform more soil organic N, nitrite, and ammonia into nitrate through nitrification[69,71]. The lower nitrate concentration in deep groundwater may be influenced by multiple factors. DO concentrations decreased with increasing depth (Fig. 6c), leading to anoxic conditions that enhanced denitrification, which could lower nitrate concentrations in deep groundwater[24]. This was further supported by the significant positive correlation between $\delta^{15}N\text{-}NO_3^-$ and $\delta^{18}O\text{-}NO_3^-$ (Fig. S7). However, reducing minerals, such as pyrite, can also chemically react with nitrates, contributing to nitrate reduction in deeper groundwater. Therefore, further research is required to fully understand the relative contributions of denitrification and reducing minerals to nitrogen removal from deep groundwater. Nitrate accumulation in deep groundwater (50–100 m) is generally higher than that in medium groundwater (20–50 m) (Fig. S8 and Table S1), indicating that groundwater nitrogen pollution in China is no longer limited to shallow layers, but gradually accumulates in deep layers[27]. Therefore, different strategies are required to remediate nitrogen pollution at different depths.

The mixing of different sources and biogeochemical processes regulates nitrate concentrations and its isotopic composition[72]. The variation pattern of nitrate concentrations and their isotopes with aquifer depth further highlights the crucial role of biological activity in nitrogen dynamics (Fig. 3). Specifically, more anoxic conditions and lower DOC (Fig. 6c, d and Fig. S2) in groundwater with increasing depth can explain the increase in $\delta^{15}N\text{-}NO_3^-$ by denitrification in the early stage of the previous period (Fig. 3d), which is consistent with our previous hypothesis. Note the negligible impact of MAT (Fig. 1c) and water temperature (Fig. 6) on nitrate concentrations. Although it has been established that temperature influences nitrate dynamics, these effects are often driven by biological activities mediated by microbes[73]. In deeper subsurface, where microbial activity is scarce, temperature effects may drop to their minimum, as indicated here[74,75]. In addition, the change in groundwater temperature from shallow to deep layers was small (Fig. 6e), such that the water temperature was not an influential factor in determining groundwater N cycling.

Implications and uncertainties

This study explored the drivers of mean nitrate concentration in groundwater at different aquifer depths under gradients of climate, geographical factors and anthropogenic activities in China. Results revealed the predominant role of aquifer depth in determining nitrate dynamics across China, offering valuable recommendations for groundwater quality management in China and globally. However, it is important to note that the datasets of land use types, ecoregions, and population density were derived from remote sensing data, which inevitably contain some errors and uncertainties[76]. In addition, although the groundwater nitrate dataset was compiled as extensively as possible, there remains a lack of representative samples from the Qinghai-Tibet Plateau. Therefore, targeted studies in this region should be conducted in the future to enhance statistical significance, thereby strengthening the validity of findings.

These wells connect the ground surface and underground, providing an opportunity to investigate the impacts of anthropogenic activities on subsurface systems. However, the role of aquifer depth in nitrate dynamics and cycling processes remains largely unexplored, especially with regard to groundwater biogeochemical processes[36]. Despite the consensus that shallow groundwater is more susceptible to nitrogen contamination, this study found that deep groundwater tends to be distributed in lowlands with high population densities, thereby increasing the risk of future contamination and leading to nitrogen enrichment in deep groundwater. Hence, controlling the nitrogen input is a primary strategy for managing global groundwater quality. Moreover, considering the coexistence of deep groundwater and high nitrate concentration in northern China (Fig. 1), more effective nitrogen management policies should be implemented to address the dual challenge of maintaining underground ecosystem stability and protecting groundwater quality, including strengthening control over both point source and non-point source pollution[70]. Note that nitrogen pollution control is a long-term process that does not yield immediate results due to

the presence of legacy nitrogen, particularly in regions with deeper aquifers. According to Van Meter et al.[18], even with 100% effective nitrogen use, it would take decades to achieve the nitrogen loading target in the Gulf of Mexico because of legacy nitrogen. In general, comprehensive measures and countermeasures should be proposed to strengthen the supervision and management of groundwater system[77,78]. The environmental capacity for industrial development and land use changes must be fully considered to ensure the protection of underground ecosystems, promote sustainable development, reduce wastewater discharge, and improve nitrogen use efficiency.

This study revealed that nitrate dynamics were highly correlated with aquifer depth, geographical factors, and climatic factors. These findings provide insight into the vulnerability of shallow groundwater to nitrate contamination and the slow and unsatisfactory nature of remediation. In addition, our analyses revealed the frequently overlooked impact of aquifer depth on the strength of the nitrogen cascade[79]. That is, nitrogen cascade strength depends on groundwater biogeochemical processes, which are linked to aquifer depth. Considering the high cost of nitrogen removal, especially for groundwater, more carefully controlled experiments are imperative to authenticate this inference and control mechanism that was previously proposed. Undoubtedly, future Water Pollution Prevention and Control Law of China should adopt more flexible management strategies for groundwater water quality and prioritize inter-regional cooperation to effectively address the escalating nitrogen loading in groundwater.

Materials and methods

Data collection

Groundwater nitrate concentration and isotope data (including NO_3^-, $\delta^{15}N\text{-}NO_3^-$, and $\delta^{18}O\text{-}NO_3^-$) from a total of 4047 groundwater sites in China were compiled from available published papers since 2000 (Fig. 1 and supplemental data). Spring data were collected at a depth of 0 m. Several other parameters, including longitude, latitude, groundwater aquifer depth, total dissolved solids (TDS), electrical conductivity (EC), water temperature (T-water), pH, dissolved oxygen (DO), dissolved organic carbon (DOC), and Oxidation-Reduction Potential (Eh) were also included. To ensure data reliability, significant outliers (below the first quartile minus 1.5 × interquartile range (IQR) or above the third quartile plus 1.5 × IQR) were excluded during the process of data processing[80]. To ensure the dataset covers the gradients of geographical, climatic, and human factors, we incorporated data from regions with diverse elevations, distinct climate zones, varied land use types, and population densities. This allowed us to capture wide-ranging groundwater conditions, facilitating a thorough analysis of spatial and environmental variability. Groundwater was grouped into four concentration levels according to drinking water standards of nitrate: <10 mg L^{-1} (excellent), 10–20 mg L^{-1} (good), 20–45 mg L^{-1} (medium), and >45 mg L^{-1} (poor). In addition, groundwater aquifer depth was divided into four groups[31]: <20 m (shallow), 20–50 m (medium), 50–100 m (deep), and >100 m (very deep) (Table S1). The country is grouped into eight economic regions based on economic development and geographical conditions[4], including North Coast (NC), Middle of Yellow River (MYR), North East (NE), South West (SW), East Coast (EC), North West (NW), Middle of Changjiang River (MCR), and South Coast (SC), as shown in Fig. S9.

The classification of ecoregions was based on distinct ecological, climatic, and topographical characteristics and elevation ranges, as defined by the Environmental Protection Agency of United States[81,82] (Table S6 and Fig. 1a). Lowlands (elevation ≤ 500 m) are typically flat with naturally fertile soils and well-developed drainage systems, making them suitable for agricultural activities and urban development (Land use percentage of groundwater samples: natural (15.6%), cropland (51.8%), and urban (32.6%)). Middlelands (500 <elevation ≤1500 m) have more moderate slopes and soils, supporting a mix of agriculture, forestry, and urban development but with less intensity compared to lowlands (Land use percentage of groundwater samples: natural (41.8%), cropland (42.0%), and urban (16.2%)). Finally, highlands (elevation >1500 m) are characterized by steep slopes and poorly developed soils, making them generally unsuitable for agriculture or urbanization (Land use percentage of groundwater samples: natural (75.7%), cropland (17.6%), and urban (6.7%)). The elevation data were obtained from the Ecological Forecasting Lab of National Aeronautics and Space Administration (NASA) Ames Research Center (http://ecocast.arc.nasa.gov/) with a spatial resolution of 1 km × 1 km (Table S6 and Fig. S10). The land use types were mainly divided into natural, cropland, and urban areas (Fig. S11), and the average population density from 2000 to 2020 was divided into four categories according to the quartile method of sampling site distribution: <56-person km^{-2} (low), 56–316-person km^{-2} (medium), 316–956-person km^{-2} (high), >956-person km^{-2} (very high) (Table S6 and Fig. S12). Data with a spatial resolution of 1 km × 1 km were obtained from the Data Center for Resources and Environmental Sciences, Chinese Academy of Sciences (RESDC) (http://www.resdc.cn). The mean annual precipitation (Fig. S13) and mean annual temperature (Fig. S14) for 1982–2015 were obtained from the China Meteorological Administration (CMA) (http://data.cma.cn/) with a spatial resolution of 0.25° × 0.25°. The data of agricultural N fertilizer usage and total sown region of crops, and the discharge of TN wastewater and ammonia wastewater were obtained from the National Bureau of Statistics of the People's Republic of China (http://www.stats.gov.cn).

Statistical analysis

Random forest model. As an integrated machine learning method and bagging algorithm, the random forest can effectively quantify the relative importance of each factor to reveal potential influence mechanisms[68]. RF model has been frequently applied in environmental science to map nitrate distributions and identify key influencing factors and control mechanisms. In this study, 66 spatially continuous environmental variables that may be directly or indirectly related to nitrate accumulation in groundwater were combined as potential predictors (Table S2). The principle of prediction uncertainty was calculated by the Bootstrap method by generating different Bootstrap samples, this study obtains various models. The differences in predictions from these models capture the uncertainty inherent in the modeling process. This method effectively quantifies how variations in the input data can lead to variations in the model outputs, thereby reflecting the uncertainty in the predictions. In addition, the RF model based on Gini index was employed to calculate the importance score of 10 variables (GW depth, TDS, EC, MAT, longitude, ecoregion, MAP, T-water, latitude, and pH) for nitrate dynamics. $VIM^{(Gini)}_j$ represents the score statistic for variable X_j, indicating the average impurity of node splits for the j_{th} variable across all trees in RF. The Gini index is calculated as follows:

$$GI_m = \sum_{k=1}^{K} \hat{p}_{mk}\left(1 - \hat{p}_{mk}\right) \quad (1)$$

Where K represents the number of categories in the dataset, and $\hat{p}_{mk}$ represents the estimated probability that samples in node m belong to category k. The importance of variable X_j at node m, i.e., the change in Gini index before and after the split at node m was calculated as follows:

$$VIM^{(Gini)}_{jm} = GI_m - GI_l - GI_r \quad (2)$$

Where GI_l and GI_r represent the Gini indices of the two new nodes created by the split at node. If variable X_j appears M times in the i_{th} tree, then the importance of variable X_j was calculated by:

$$VIM^{(Gini)}_{ij} = \sum_{m=1}^{M} VIM^{(Gini)}_{jm} \quad (3)$$

Therefore, the Gini importance of X_j was calculated by:

$$VIM_j^{(Gini)} = \frac{1}{n}\sum_{i=1}^{n} VIM_{ij}^{(Gini)} \quad (4)$$

Where *n* represents the number of categories trees in RF. In this study, regression prediction analysis of RF model was performed using the "rfPermute" package in R v.4.3.2 to explore the relative effects of various factors on nitrate concentration.

MixSIAR model. We also applied the Bayesian stable isotope mixing model (MixSIAR) with a Markov chain Monte Carlo (MCMC) algorithm to estimate the relative contributions of different NO_3^- sources to groundwater[38]. The calculation formula is as follows:

$$X_{ij} = \sum_{k=1}^{k} P_k\left(S_{jk} + C_{jk}\right) + \varepsilon_{ij} \quad (5)$$

$$S_{jk} \sim N\left(\mu_{jk}, \omega_{jk}^2\right) \quad (6)$$

$$C_{jk} \sim N\left(\lambda_{jk}, \tau_{jk}^2\right) \quad (7)$$

$$\varepsilon_{jk} \sim N\left(0, \sigma_{jk}^2\right) \quad (8)$$

where X_{ij} represents the δ values of isotope j of mixture measurements i (i = 1, 2, 3, …., N and j = 1, 2, 3, …., J); P_k represents the proportion of source k; S_{jk} represents the δ values of isotope j^{th} from the k^{th} source, which follows the normal distribution with the mean μ_{jk} variance and standard deviation (SD) ω_{jk}; C_{jk} represents the fractionation coefficient of j isotope from the k^{th} source, which follows the normal distribution with the mean λ_{jk} and SD τ_{jk}; ε_{jk} is the residual error representing the additional unquantifiable variance between individual mixtures, which follows the normal distribution with the mean 0 and SD σ_{jk}. More detailed information on MixSIAR model is referred to Ren et al.[58] and Fadhullah et al.[40]. Note, the typical end-number isotopic values of atmospheric deposition, manure & sewage, soil nitrogen, and chemical fertilizer, and the fractionation factor (Ɛ) used in the MixSIAR model are derived from the relevant literature on data collection (Table S3). The transport pathways of manure and sewage differ, with sewage often reaching groundwater through leaching or leaking pipes and manure typically through agricultural runoff. However, manure and sewage have overlapping isotopic signatures, which make it challenging to differentiate them. We therefore group 'manure & sewage' in one class, as similarly done in literature[41,83]. In this study, MixSIAR model was conducted using R software with the "MixSIAR" package to quantify the categories of different sources of NO_3^-.

We further used a few other analysis/visualization tools. Statistical relationships among nitrate dynamics, climate conditions, geography, and anthropogenic activities were examined by one-way analysis of variance (ANOVA) using Tukey's Honestly Significant Difference test[13]. The Sankey diagram, composed of nodes (each variable) and connecting lines, shows the process of nitrate enrichment caused by influencing factors and the organic integration of related parameter data and was therefore used to visualize nitrogen sources[84]. Decision tree-heatmap is a comprehensive visualization method that integrates decision trees and heatmaps[85]. It used the data as a heatmap of the tree's leaf nodes and integrates the tree structure to effectively explain how the tree nodes segment the feature space and their execution methods. The decision tree-heatmap can also reveal the correlation structure of the data and the importance of each feature. Here, we used decision-tree heatmaps to predict the threshold values of different nitrate concentrations using the "treeheatr" package based on the interactions among aquifer depth, population density, land use, and ecoregion characteristics. In addition, the structural equation model was used to explore the regularity of nitrate dynamics under different geographical and climate factors[46]. Structural equation modeling is hypothesis driven, focusing on causal relationships and the direct, indirect, and total effects between variables through path coefficients. It is well suited for validating theoretical frameworks and understanding the mechanisms behind variable interactions. In this study, auxiliary data (including geographical (including ecoregion, latitude, and longitude), climate factors (including MAP and MAT), hydrochemical characteristics (including TDS, pH, EC, and T-water)), and aquifer depth were set as the variables. Correlations and contributions between variables were analyzed using Amos software[86].

Reporting summary

Further information on research design is available in the Nature Portfolio Reporting Summary linked to this article.

Data availability

All raw data used is publicly accessible and linked in the manuscript. The Chinese groundwater datasets and its references available are accessible https://doi.org/10.6084/m9.figshare.28103579, and processed datasets of Table S1–S6 are freely accessible https://doi.org/10.6084/m9.figshare.28103579.

Code availability

Processed codes of random forest and MixSIAR model are freely accessible at https://doi.org/10.5281/zenodo.14565555.

Received: 28 July 2024; Accepted: 9 January 2025;
Published online: 28 January 2025

References

1. Fukuda, S., Noda, K. & Oki, T. How global targets on drinking water were developed and achieved. *Nat. Sustainability* **2**, 429–434 (2019).
2. Scanlon, B. R. et al. Global water resources and the role of groundwater in a resilient water future. *Nat. Rev. Earth Environ.* **4**, 87–101 (2023).
3. Wang, M. et al. Accounting for interactions between Sustainable Development Goals is essential for water pollution control in China. *Nat. Commun.* **13**, 730 (2022).
4. Liu, M. et al. Spatial assessment of tap-water safety in China. *Nat. Sustainability* **5**, 689–698 (2022).
5. Werner, A. H. & Gleeson, T. Regional strategies for the accelerating global problem of groundwater depletion. *Nat. Geosci.* **5**, 853–861 (2012).
6. Gleeson, T., Befus, K. M., Jasechko, S., Luijendijk, E. & Cardenas, M. B. The global volume and distribution of modern groundwater. *Nat. Geosci.* **11**, 542 (2016).
7. Ministry of Water Resources. Statistical bulletin on China water activities 2021. (2022).
8. McDonough, L. K. et al. Changes in global groundwater organic carbon driven by climate change and urbanization. *Nat. Commun.* **11**, 1279 (2020).
9. Gu, B. J., Ge, Y., Chang, S. X., Luo, W. D. & Chang, J. Nitrate in groundwater of China: Sources and driving forces. *Glob. Environ. Change* **23**, 1112–1121 (2013).
10. Ebeling, P. et al. QUADICA: Water quality, discharge and catchment attributes for large-sample studies in Germany. *Earth Syst. Sci. Data* **14**, 3715–3741 (2022).
11. Suthar, S. et al. Nitrate contamination in groundwater of some rural areas of Rajasthan, India. *J. Hazard. Mater.* **171**, 189–199 (2009).
12. Jurgens, B. C. et al. Over a third of groundwater in USA public-supply aquifers is Anthropocene-age and susceptible to surface contamination. *Commun. Earth Environ.* **3**, 153 (2022).
13. Ioannis, M., Leonard, I., Lucilena, R., Jason, J. & Daren, C. Global patterns of nitrate isotope composition in rivers and adjacent aquifers reveal reactive nitrogen cascading. *Commun. Earth Environ.* **2**, 52 (2021).

14. Abascal, E., Gómez-Coma, L., Ortiz, I. & Ortiz, A. Global diagnosis of nitrate pollution in groundwater and review of removal technologies. *Sci. Total Environ.* **810**, 152233 (2022).
15. Kanter, D. R., Chodos, O., Nordland, O., Rutigliano, M. & Winiwarter, W. Gaps and opportunities in nitrogen pollution policies around the world. *Nat. Sustainability* **3**, 956–963 (2020).
16. Rockström, J. et al. Safe and just Earth system boundaries. *Nature* **619**, 102–111 (2023).
17. Morrissy, J. G. et al. Nitrogen contamination and bioremediation in groundwater and the environment: A review. *Earth Sci. Rev.* **222**, 103816 (2021).
18. Van Meter, K. J., Van Cappellen, P. & Basu, N. B. Legacy nitrogen may prevent achievement of water quality goals in the Gulf of Mexico. *Science* **360**, 427–430 (2018).
19. Yu, C. et al. Managing nitrogen to restore water quality in China. *Nature* **567**, 516–520 (2019).
20. Houlton, B. Z., Morford, S. L. & Dahlgren, R. A. Convergent evidence for widespread rock nitrogen sources in Earth's surface environment. *Science* **360**, 58–62 (2018).
21. Reay, D. S., Dentener, F., Smith, P., Grace, J. & Feely, R. A. Global nitrogen deposition and carbon sinks. *Nat. Geosci.* **1**, 430–437 (2008).
22. Ma, T. et al. Pollution exacerbates China's water scarcity and its regional inequality. *Nat. Commun.* **11**, 650 (2020).
23. Merder, J. et al. Geographic redistribution of microcystin hotspots in response to climate warming. *Nat. Water* **1**, 844–854 (2023).
24. Zhi, W., Ouyang, W., Shen, C. & Li, L. Temperature outweighs light and flow as the predominant driver of dissolved oxygen in US rivers. *Nat. Water* **1**, 249–260 (2023).
25. Galloway, J. N. et al. Nitrogen cycles: Past, present, and future. *Biogeochemistry* **70**, 153–226 (2004).
26. Xu, P. et al. Fertilizer management for global ammonia emission reduction. *Nature* **198**, 5592 (2024).
27. Ascott, M. J. et al. Global patterns of nitrate storage in the vadose zone. *Nat. Commun.* **8**, 1416 (2017).
28. Wang, S. et al. Nitrogen stock and leaching rates in a thick vadose zone below areas of long-term nitrogen fertilizer application in the North China Plain: a future groundwater quality threat. *J. Hydrol.* **576**, 28–40 (2019).
29. Liu, X. et al. Impact of groundwater nitrogen legacy on water quality. *Nat. Sustainability* **7**, 891–900 (2024).
30. Niu, X. et al. Tracing the sources and fate of NO_3^- in the vadose zone-groundwater system of a thousand-year-cultivated region. *Environ. Sci. Technol.* **56**, 9335–9345 (2022).
31. Moeck, C. et al. A global-scale dataset of direct natural groundwater recharge rates: A review of variables, processes and relationships. *Sci. Total Environ.* **717**, 137042 (2020).
32. Li, L. et al. Climate control on river chemistry. *Earth's. Future* **10**, e2021EF002603 (2022).
33. Sadayappan, K., Kerins, D., Shen, C. & Li, L. Riverine nitrate concentrations predominantly driven by human, climate, and soil property in the Contiguous United States. *Water Res* **226**, 119295 (2022).
34. Chen, L. et al. Global distribution of mercury in foliage predicted by machine learning. *Environ. Sci. Technol.* **58**, 15629–15637 (2024).
35. Castaldo, G., Visser, A., Fogg, G. E. & Harter, T. Effect of groundwater age and recharge source on nitrate concentrations in domestic wells in the San Joaquin valley. *Environ. Sci. Technol.* **55**, 2265–2275 (2021).
36. Szymczycha, B., Kroeger, K. D., Crusius, J. & Bratton, J. F. Depth of the vadose zone controls aquifer biogeochemical conditions and extent of anthropogenic nitrogen removal. *Water Res* **123**, 794–801 (2017).
37. Nizzoli, D., Welsh, D. T. & Viaroli, P. Denitrification and benthic metabolism in lowland pit lakes: The role of trophic conditions. *Sci. Total Environ.* **703**, 134804 (2020).
38. Kim, S. H. et al. Systematic tracing of nitrate sources in a complex river catchment: An integrated approach using stable isotopes and hydrological models. *Water Res* **235**, 119755 (2023).
39. Carrey, R. et al. Combining multi-isotopic and molecular source tracking methods to identify nitrate pollution sources in surface and groundwater. *Water Res* **188**, 116537 (2021).
40. Fadhullah, W. et al. Nitrate sources and processes in the surface water of a tropical reservoir by stable isotopes and mixing model. *Sci. Total Environ.* **700**, 134517 (2020).
41. Kendall, C., Elliot, E. M. & Wankel, S. D. Tracing anthropogenic inputs of nitrogen to ecosystems. In: Michener, R., Lajtha, K. (Eds.), *Stable Isotopes in Ecology and Environmental Science, second ed. Blackwell Publishing Ldt, Oxford*, *pp*. 375-449. (2007).
42. Kim, M. S. et al. Innovative approach to reveal source contribution of dissolved organic matter in a complex river watershed using end-member mixing analysis based on spectroscopic proxies and multi-isotopes. *Water Res*. **230**, 119470 (2023).
43. Li, Q. K. et al. Impacts of sewage irrigation on soil properties of a farmland in China: A review. *Phyton-Int. J. Exp. Bot.* **87**, 40–50 (2018).
44. Kou, X. et al. Tracing nitrate sources in the groundwater of an intensive agricultural region. *Agric. Water Manag.* **250**, 106826 (2021).
45. Zhang, H., Xu, Y., Cheng, S., Li, Q. & Yu, H. Application of the dual-isotope approach and Bayesian isotope mixing model to identify nitrate in groundwater of a multiple land-use area in Chengdu Plain. *China Sci. Total Environ.* **717**, 137134 (2020).
46. Elrys, A. S. et al. Expanding agroforestry can increase nitrate retention and mitigate the global impact of a leaky nitrogen cycle in croplands. *Nat. Food* **4**, 109–121 (2023).
47. Li, S. L. et al. Nitrogen dynamics in the Critical Zones of China. *Prog. Phys. Geogr.: Earth Environ.* **46**, 869–888 (2022).
48. Sebilo, M., Mayer, B., Nicolardot, B. & Pinay, G. Long-term fate of nitrate fertilizer in agricultural soils. *Proc. Natl Acad. Sci.* **110**, 18185–18189 (2013).
49. Möbius, J. Isotope fractionation during nitrogen remineralization (ammonification): Implications for nitrogen isotope biogeochemistry. *Geochim. Cosmochim. Acta* **105**, 422–432 (2013).
50. Schlesinger, W. H. On the fate of anthropogenic nitrogen. *Proc. Natl Acad. Sci.* **106**, 203–208 (2009).
51. Rachel, E. M. et al. Evidence, causes, and consequences of declining nitrogen availability in terrestrial ecosystems. *Science* **376**, eabh3767 (2022).
52. Kumar, R. et al. Strong hydroclimatic controls on vulnerability to subsurface nitrate contamination across Europe. *Nat. Commun.* **11**, 6302 (2020).
53. Ehrhardt, S. et al. Nitrate transport and retention in western European catchments are shaped by hydroclimate and subsurface properties. *Water Resour. Res.* **57**, e2020WR029469 (2021).
54. Benettin, P., Fovet, O. & Li, L. Nitrate removal and young stream water fractions at the catchment scale. *Hydrol. Process.* **34**, 2725–2738 (2020).
55. Ma, Z. et al. Agricultural nitrate export patterns shaped by crop rotation and tile drainage. *Water Res*. **229**, 119468 (2023).
56. Munz, M., Oswald, S. E., Schäfferling, R. & Lensing, H. J. Temperature-dependent redox zonation, nitrate removal and attenuation of organic micropollutants during bank filtration. *Water Res.* **162**, 225–235 (2019).
57. Yue, F. et al. Rainfall and conduit drainage combine to accelerate nitrate loss from a karst agroecosystem: Insights from stable isotope tracing and high-frequency nitrate sensing. *Water Res.* **186**, 116388 (2020).
58. Ren, K. et al. Nitrate sources and nitrogen dynamics in a karst aquifer with mixed nitrogen inputs (Southwest China): Revealed by multiple stable isotopic and hydro-chemical proxies. *Water Res*. **210**, 118000 (2022).

59. Gao, D. et al. Responses of soil nitrogen and phosphorus cycling to drying and rewetting cycles: A meta-analysis. *Soil Biol. Biochem.* **148**, 107896 (2020).
60. Long, D. et al. South-to-North water diversion stabilizing Beijing's groundwater levels. *Nat. Commun.* **11**, 3665 (2020).
61. Nakagawa, K., Amano, H., Persson, M. & Berndtsson, R. Spatiotemporal variation of nitrate concentrations in soil and groundwater of an intensely polluted agricultural area. *Sci. Rep.* **11**, 2598 (2021).
62. Zhi, W. & Li, L. The shallow and deep hypothesis: subsurface vertical chemical contrasts shape nitrate export patterns from different land uses. *Environ. Sci. Technol.* **54**, 11915–11928 (2020).
63. Hansen, B., Thorling, L., Schullehner, J., Termansen, M. & Dalgaard, T. Groundwater nitrate response to sustainable nitrogen management. *Sci. Rep.* **7**, 8566 (2017).
64. Zhang, X. et al. Quantification of global and national nitrogen budgets for crop production. *Nat. Food* **2**, 529–540 (2021).
65. Zhang, X., Davidson, E. A., Mauzerall, D. L. & Searchinger, T. D. Managing nitrogen for sustainable development. *Nature* **528**, 51–59, (2015).
66. Huang, J. et al. Characterizing the river water quality in China: Recent progress and on-going challenges. *Water Res.* **201**, 117309 (2021).
67. Liu, X., Yue, F. J., Wong, W. W., Guo, T. L. & Li, S. L. Unravelling nitrate transformation mechanisms in karst catchments through the coupling of high-frequency sensor data and machine learning. *Water Res.* **267**, 122507 (2024).
68. Basu, N. B., Dony, J., Van Meter, K. J., Johnston, S. J. & Layton, A. T. A random forest in the great lakes: Stream nutrient concentrations across the transboundary great lakes basin. *Earth's. Future* **11**, e2021EF002571 (2023).
69. Turkeltaub, T., Kurtzman, D. & Dahan, O. Real-time monitoring of nitrate transport in the deep vadose zone under a crop field-implications for groundwater protection. *Hydrol. Earth Syst. Sci.* **20**, 3099–3108 (2016).
70. Basu, N. B. et al. Managing nitrogen legacies to accelerate water quality improvement. *Nat. Geosci.* **15**, 97–105 (2022).
71. Wheeler, D. C., Nolan, B. T., Flory, A. R., DellaValle, C. T. & Ward, M. H. Modeling groundwater nitrate concentrations in private wells in Iowa. *Sci. Total Environ.* **536**, 481–488 (2015).
72. Kumar, A., Ajay, A., Dasgupta, B., Bhadury, P. & Sanyal, P. Deciphering the nitrate sources and processes in the Ganga river using dual isotopes of nitrate and Bayesian mixing model. *Environ. Res.* **216**, 114744 (2023).
73. Saghaï, A., Pold, G., Jones, C. M. & Hallin, S. Phyloecology of nitrate ammonifiers and their importance relative to denitrifiers in global terrestrial biomes. *Nat. Commun.* **14**, 8249 (2023).
74. Palacios, D. M., Hazen, E. L., Schroeder, I. D. & Bograd, S. J. Modeling the temperature-nitrate relationship in the coastal upwelling domain of the California Current. *J. Geophys. Res.: Oceans* **118**, 3223–3239 (2013).
75. Greaver, T. L. et al. Key ecological responses to nitrogen are altered by climate change. *Nat. Clim. Change* **6**, 836–843 (2016).
76. Duan, H. et al. Quantification of diffusive methane emissions from a large eutrophic lake with satellite imagery. *Environ. Sci. Technol.* **57**, 13520–13529 (2023).
77. Liu, X., Yue, F., Guo, T. & Li, S. High-frequency data significantly enhances the prediction ability of point and interval estimation. *Sci. Total Environ.* **912**, 169289 (2024).
78. Zhi, W., Appling, A. P., Golden, H. E., Podgorski, J. & Li, L. Deep learning for water quality. *Nat. Water* **2**, 228–241 (2024).
79. Galloway, J. N., Aber, J. D., Erisman, J. W. & Seitzinger, S. P. The nitrogen cascade. *Bioscience* **53**, 341–356 (2003).
80. Zhi, W., Klingler, C., Liu, J. & Li, L. Widespread deoxygenation in warming rivers. *Nat. Clim. Change* **13**, 1105–1113 (2023).
81. Herlihy, A. T. et al. Striving for consistency in a national assessment: The challenges of applying a reference-condition approach at a continental scale. *J. North Am. Benthol. Soc.* **27**, 860–877 (2008).
82. De Blij, H. J. Geography: Regions and concepts, *2nd ed*. *Wiley & Sons*, *New York*. (1978).
83. Xue, D. et al. Present limitations and future prospects of stable isotope methods for nitrate source identification in surface- and groundwater. *Water Res.* **43**, 1159–1170 (2009).
84. Jayanthi, M. et al. Ecosystem characteristics and environmental regulations based geospatial planning for sustainable aquaculture development. *Land Degrad. Dev.* **31**, 2430–2445 (2020).
85. Le, T. T. & Moore, J. H. Treeheatr: An R package for interpretable decision tree visualizations. *Bioinformatics* **37**, 282–284 (2020).
86. Lv, M. et al. Human impacts on polycyclic aromatic hydrocarbon distribution in Chinese intertidal zones. *Nat. Sustainability* **3**, 878–884 (2020).

Acknowledgements

This work was supported by the National Natural Science Foundation of China [Grant number 41925002] and [Grant numbers: 42221001; 42293262; 42073076]; Key Technologies Research and Development Program of China [2023YFF0806001; 2024YFD1701102], and financial support was provided by the Haihe Laboratory of Sustainable Chemical Transformations, and China Scholarship Council. We confirm that no specific permissions were required for the sampling carried out in this study. The list of referenced data can be found in the Supplementary References.

Author contributions

X.L.: Conceptualization, Methodology, Software, Visualization, Writing-original draft. F.-J.Y.: Conceptualization, Data curation, Methodology, Funding, Supervision, Validation, Writing-review & editing. L.L.: Methodology & Writing-review. F.Z.: Methodology & Writing-review. H.W.: Methodology & Writing-review. Z.Y.: Methodology & Writing-review. L.W.: Methodology & Writing-review. W.W.W.: Conceptualization, Data curation, Methodology, Supervision, Validation, Writing-review & editing. C.-Qi.L.: Methodology & Writing-review. S.-L.L.: Methodology, Funding, Supervision, Writing-review & editing.

Competing interests

The authors declare no competing interests.

Additional information

Supplementary information The online version contains supplementary material available at https://doi.org/10.1038/s43247-025-02016-7.

Correspondence and requests for materials should be addressed to Fu-Jun Yue or Si-Liang Li.

Peer review information *Communications Earth & Environment* thanks Alexander Bouwman and the other, anonymous, reviewer(s) for their contribution to the peer review of this work. Primary Handling Editors: Somaparna Ghosh. A peer review file is available.